Synthesis of nanostructured metal oxides for their use in gas sensors

Author: Lluís Agulló i Manobens.
Advisor: Paolo Pellegrino
Facultat de Física, Universitat de Barcelona, Diagonal 645, 08028 Barcelona, Spain.*

Abstract: Gallium oxide (Ga_2O_3) nanowires (NW) were successfully grown using the Vapour-Liquid-Solid method from a metallic source and were later characterized by means of Scanning Electron Microscopy (SEM). X-ray diffraction, SEM and photoluminescence (PL) data from previously grown mixed indium oxide (In_2O_3) and Ga_2O_3 nanowires were also analysed. From the analysis of the Ga_2O_3 nanowires, a severe hindering effect of a marginal concentration of oxygen on the carrier gas mix was observed regarding the synthesis. For the mixed nanowires, an additional PL band to the main direct band-to-band transition was observed in photoluminescence, which may be attributed to optical transitions from surface states located at the outer shell of the nanowires, and possibly involving impurities such as Ga and C. In addition, a coherent shift was observed of both PL bands, probably caused by changes in the dimensions of the crystalline domains.

I. INTRODUCTION

Due to their high sensitivity to certain gases and low cost [1], metal oxides have become a common active material in solid state gas sensing devices.

Upon interaction with the target gas, the electrical variations these materials undergo take place almost exclusively at the surface, as the oxidized surface easily interacts with both reducing and oxidising gases [1], thus geometries that enhance the surface-to-volume ratio are usually sought for. In that regard, the use of 2D and 1D nanometric structures (i.e., thin films and nanowires and nanotubes) has been proven successful, allowing for reliable devices capable of responding to gas concentrations down to few ppb in a matter of minutes[2]. Furthermore, the nanometric nature of such structures notably reduces power consumption if they require to function at temperatures above 150ºC.

The choice of available metal oxides to be used for such devices is vast. Gallium and indium oxides, both wide band-gap semiconducting oxides of group III elements, have shown a good performance as gas sensors when in nanowire (NW) shape.

There is a large number of methods to grow 1D metal oxide structures. Among them, chemical vapor deposition techniques are widely used due to their consistent results. More specifically, for the growth of NWs, the vapour liquid solid (VLS) method, and its variations are a commonly used [3].

Recently, the UB-MIND research group has noticed that the use of non pure metallic sources, such as a mix of metal oxide powder and graphite, can contaminate the NWs. Although such contamination can provide an additional degree of freedom for gas sensing, it does not allow the simultaneous growth of heterostructures of different oxides, so that the search for the correct conditions to grow carbon-free metal oxide nanowires is an open issue addressed in this work.

In addition, it has been noticed in past experiments that, when growing mixed gallium and indium oxides from a source consisting on a mixed powder of both metals' oxides and graphite, the evaporation rate of gallium is so low that its presence in the resulting nanostructures is marginal. An attempt to tackle down this issue was carried out in this work as well.

II. EXPERIMENTAL PROCEDURE

A. NWs growth

Gallium oxide NWs were grown using the VLS method. This method consists in evaporating the precursor material and dragging it, with the help of a carrier gas, to the substrate where the NWs growth will occur. On the substrate's surface, nanodroplets of gold will act as a catalyser that captures the metal oxide molecules and generates the NWs once it supersaturates by precipitation at the interface between the droplet and substrate.

In our case, the procedure was carried inside a quartz tube with a diameter of 5cm, in which a series of alumina supports containing the source and the substrates were inserted. The tube itself is inserted in a Lindbergh furnace, which allows to set different temperatures for each of the three different regions of the central part of the tube. At the beginning the temperature was gradually risen from room temperature up to 800/800/650 ºC, in downstream order, in a span of 52 minutes. Once the target temperatures were reached, they were kept for an hour with a constant gas flow, and after that the heating was turned off, letting the samples cool down during 2 hours under constant Argon flow.

Gas flow was controlled by two mass flow controllers that regulated the flow of every individual gas line, connected to its respective gas bottle. Two gases were used for two different experiments: for the first one 100 sccm of Argon (purity 5.0) was used, while the same amount of a mix of argon with a 0.1% oxygen was used for the second one. Before heating the tube, the tube was vacuum pumped to remove contaminants which may interfere with the growth. .

The substrates we used were 5mm square-shaped silicon plates with a 1 μm thick SiO_2 layer, covered by 10-20 nm of gold (provided by the Centre Nacional de Microelectronica, CNM). During the heating up, the gold film melts and the gold droplets act as the liquid catalyser.

The used source was pure metallic gallium (purity 99.99%, purchased from Sigma-Aldrich). 0.494g were used in the first synthesis, which were placed in the first support, which was flipped. Two substrates were placed onto the same support, upstream from the gallium piece. The other substrates were

* Electronic address:llagullm10@alumnes.ub.edu

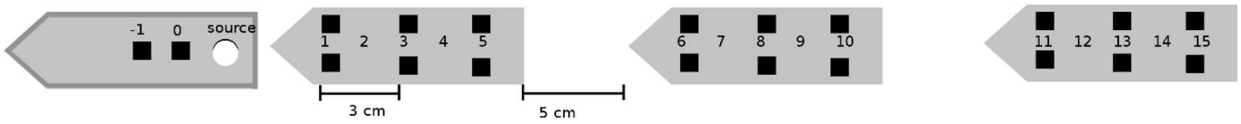

Fig 1: Sketch of the samples and source distribution in the tube. Gas flows from left to right.

placed by pairs downstream onto different supports. The precise configuration is illustrated in Fig. 1.

The procedure to grow $(In,Ga)_2O_3$ NWs was almost identical to the one for the pure Ga_2O_3 NWs. The only changes were the use of a mix of C:Ga_2O_3 source (with a 1.5:1 ratio), a flux of 100sccm of pure argon and the maximum temperature was set to 950ºC. The In source for these nanowires was leftover In (in the form of In_2O_3) from previous experiments that had solidified at the internal surface of the quartz tube. In spite of that, the likelihood of the chemical reactions required for the formation of Ga_2O_3 NWs is so low compared to that of In_2O_3 that it will still remain marginal.

The original purpose for the growth of these NWs without adding In_2O_3 in the source was to attempt to compensate for the low rate of Ga evaporation respect to the one of In_2O_3 from the C:Ga_2O_3:In_2O_3 precursor.

Two experiments of $(In,Ga)_2O_3$ NWs growth were carried out, both with the same configuration.

B. Characterization

All substrates were observed with a Jeol 7100 Field Emission Scanning Electron Microscope (SEM), operating at 15keV, providing a qualitative insight on the success of the growth on each sample. In_2O_3 samples that were considered of interest were further inspected with a PANalytical X'Pert PRO MRD X-ray diffractometer, irradiated with Ka radiation of a Cu source (wavelength: 0.15406nm), using grazing incidence to maximize the interaction volume. The same set of samples was additionally analysed by photoluminescence, using the 325nm emission of an argon laser, outputting roughly 15mW on the samples, and a monochromator coupled to a Hamamatsu photomultiplier detector.

III. RESULTS AND ANALYSIS

A. SEM.

SEM images of the Ga_2O_3 samples show that the addition of oxygen to the carrier Ar severely hindered the NWs' growth, to the extent that no NWs could be found on any of the substates. The cause of that could be the oxidation of the source material, metallic Ga, before it evaporates, which would drastically decrease the process efficiency. In the successful experiment's images a high density of nanowires of different lengths and shapes can be observed. As one can see in fig. 2, increasing the distance of the substrate from the source, the density of nanowires progressively decreases, with a sudden drop at position "3".

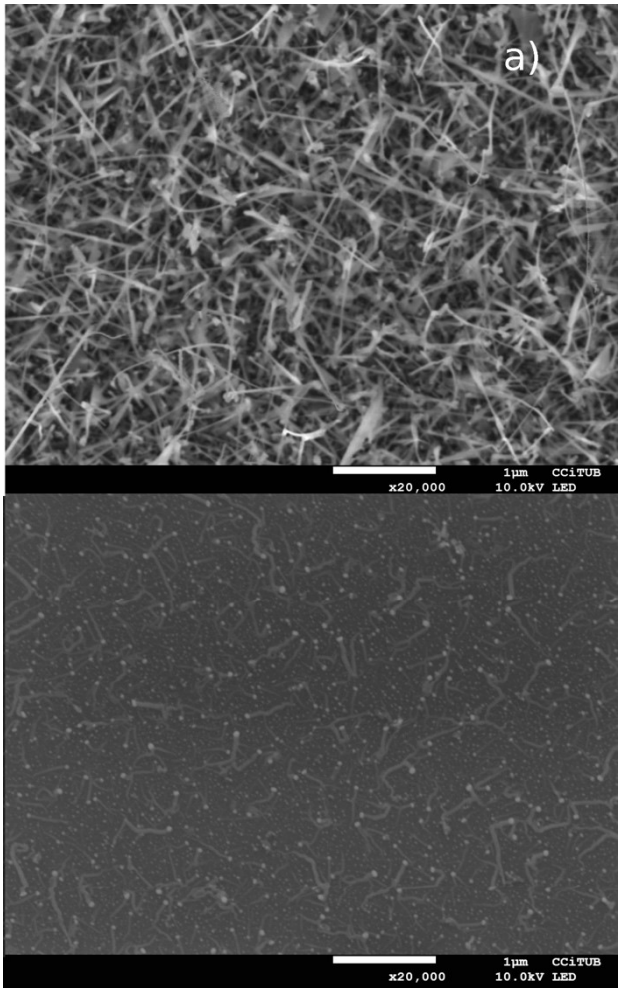

Fig 2: SEM images for (a) the closest (position "0") and (b) a far (pos. 5) sample for the non-oxygenated experiment. Isolated spheres observed in (b) are solidified gold nanodroplets.

For the In_2O_3 NWs, instead, we find a lower density of nanowires. This is not surprising, as even at those temperatures the growth of In_2O_3 and the evaporation of C: Ga_2O_3 are quite inefficient. Similarly to what was seen for Ga_2O_3 samples, one can observe a decrease in the amount of NWs the farther we are from the source. Samples grown upstream (positions "0" and "-1", such as the ones displayed in figures 3 and 4), appear to have the highest NW densities. We can observe how in the sample grown in position "0" we can find additional In_2O_3 nanocrystals growing around the nanowires. This could suggest locally a higher amount of In during the growth in those samples compared to those further upstream, as such crystals were not observed in samples in position "-1". Since the only possible source for In in those experiments was the

quartz cylinder's inner wall, which was contaminated during previous experiments, the only explanation for the unequal distribution of In during the growth would be the existence of a stronger turbulent regime in the region where these samples were placed, namely region "0".

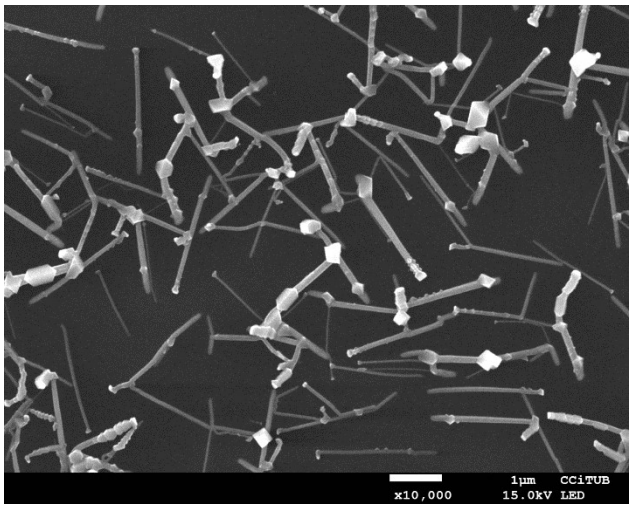

Fig 3: SEM image of a sample close to the source (pos. "0") for the $(In,Ga)_2O_3$ experiment.

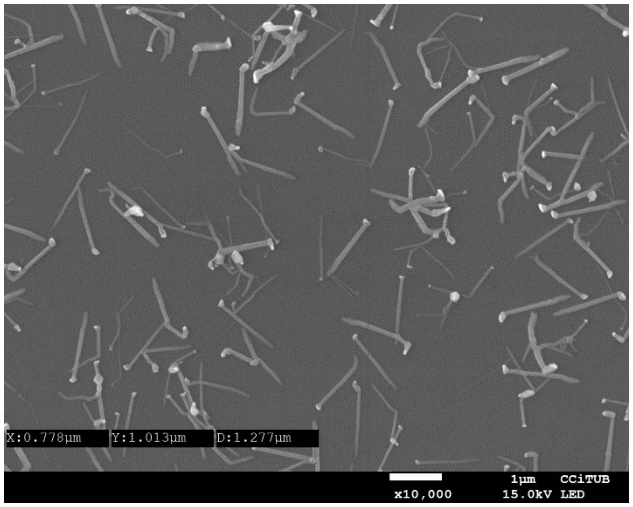

Fig 4: SEM image of a sample far from the source (pos. -1) for the $(In,Ga)_2O_3$ experiment.

B. X-ray diffraction.

The diffraction patterns for the $(In,Ga)_2O_3$ samples is shown in figure 5. A well-defined pattern of narrow lines emerges over a slowly decreasing background. Bragg's law was used to find the interplanar distance parameter of the NWs by the angle position of each line:

$$2\,d\,sin(\theta) = n\,\lambda \qquad (1)$$

where d is the interplanar distance, θ the peak's position, λ the X-ray wavelength and n the peak order.

Checking the diffraction patterns, shown in figure 5, we can assign the observed peaks to cubic In_2O_3 (JCDPS card no. 06-416). However, no characteristic peaks for monoclinic Ga_2O_3 can be seen in the figure, as they should fit to the listed card (JCDPS card no. 41-1103), which presents its most intense at 31.7º. We can therefore conclude that the Ga atoms that may have incorporated into the nanowires or other nanostructures are in substitutional In position.

To obtain the lattice parameter, we can then use the formula:

$$a = d\sqrt{h^2 + k^2 + l^2} \qquad (2)$$

Where parameters h, k and l are the Miller indexes. For the most intense cubic In_2O_3 peak, at 30.7º in our measurements, the value of $\sqrt{h^2 + k^2 + l^2}$ is 3.461016.

Having found the lattice parameter a, it was compared to the expected parameters for both In_2O_3 and Ga_2O_3, and through a linear extrapolation the gallium concentration in $(In_{1-x}Ga_x)_2O_3$ was evaluated by the Vegard's law [4]:

$$x = \frac{a_{In} - a}{a_{In} - a_{Ga}} \qquad (3)$$

where x is the gallium concentration, a is the calculated lattice parameter and a_i are the expected lattice parameters for a cubic structure made up only of one of the metal oxides. Notice however that in the case of NWs, Ga_2O_3 and In_2O_3 do not crystallise in the same space group. In order to estimate the effect of substitutional gallium, the gallium oxide lattice parameter was extrapolated from the ratio of the lattice parameters for Ga_2O_3 and In_2O_3 when crystallising in an hexagonal lattice, giving a value of 0.8753nm. The lattice parameter for In_2O_3 was calculated from the diffraction pattern obtained from an experiment in which only C:In_2O_3 was used for the source, and was found to measure 1.00983nm.

An additional information that can be extracted from the diffraction patterns is the size of the crystalline domains. This can be obtained from the peaks' width, using Scherrer's formula [5]:

$$D = \frac{K\,\lambda}{\beta\,\cos(\theta)} \qquad (4)$$

where β is the peak's full width half maximum (FWHM) and K is the shape factor, whose value is estimated to be of 0.9.

The estimated amount of Ga, as well as all other deduced parameters are displayed in Table 1 for the different $(In,Ga)_2O_3$ samples.

Sample	position	2θ(º)	β (º)	a(nm)	x(%)	D(nm)
S1	0 (exp 1)	30.662	0.372(±0.015)	1.0093	0.4(±0.5)	22.1 (±1.0)
S2	-1 (exp 1)	30.74	0.48(±0.07)	1.0075	2.3(±2)	17.4 (±2.0)
S3	0 (exp 2)	30.629	0.28(±0.05)	1.0092	-0.4(±1.4)	29.4 (±4.0)

Table 1: Measured (2θ, β) and estimated (a, x, D) parameters obtained from the XRD diffraction patterns from Fig. 5, using the values for the 30.7º peak. The position the samples were put and if they were grown on the first or second $(In,Ga)_2O_3$ experiment is also shown.

Because the diffraction was obtained using the grazing incidence configuration, the acquired patterns are considerably noisy, which means that the accuracy of the major part of the evaluated parameters is rather limited. However, they are accurate enough to confirm that the presence of Ga is marginal (less than 5%). Additionally, a tendency of higher gallium concentrations resulting in smaller crystalline domains seems to appear, however further measurements with higher signal-to-noise ratio are required to prove/confirm such a dependence.

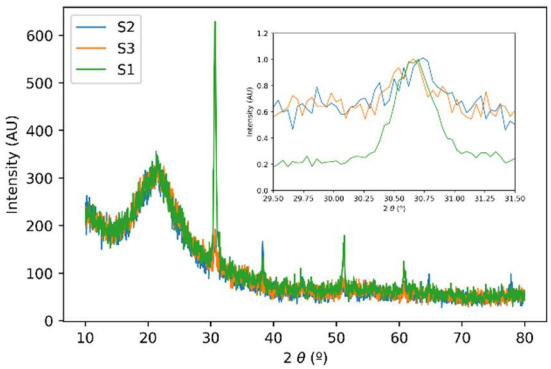

Fig 5: XRD spectra for $(In,Ga)_2O_3$ samples. A zoomed-in and normalized view of the 30.6º peak is shown in the inset.

C. Photoluminescence.

The measured PL spectra for the different $(In,Ga)_2O_3$ samples ranged from 330 to 850 nm, with the interesting region lying at wavelengths below 450 nm, as the remaining measured structures are considered just 2nd order replicas of the emission occurring at the shorter wavelengths. The results for the photoluminescence (PL) are shown in figure 6. For each spectrum, two peaks were found: a larger peak at around 3.4 eV and a smaller one at 3.1 eV, whose intensity is three to four smaller than the previous one. As can be observed in Figure 6, the energy difference of both peaks is almost constant, at a value of 312 me. However, the position of the whole spectra seem to shift between the different samples by about 50 meV.

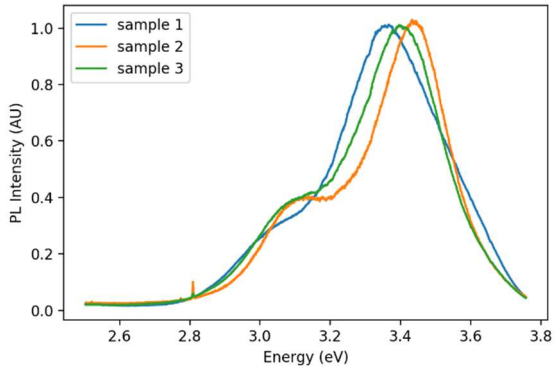

Fig 6: Observed PL spectra of the three $(In,Ga)_2O_3$ samples.

D. Discussion.

It is most likely that the most energetic PL peak is related to band-to-band transitions, as its energy is close to the bandgap value reported [6]. However, the origin of the less energetic peak is not as certain. Some authors, such as Yaiha et al. [7] have attributed this "blue" peak to non-oxidized In atoms, that may act as dopants. However, its intensity, comparable to the band to band transition, would imply that the concentration of these unreacted In ions dispersed in the oxide matrix would attain an important fraction of the atomic density of the stochiometric In_2O_3, a conclusion not supported by any other experimental evidence. On the other hand, by looking at the absorption spectra obtained by Mohamed et al. [6] in samples made under comparable conditions, it can be seen that when Ga is added in the order of 2% to an In_2O_3 sample, an additional absorption band appears just below the bandgap absorption edge. Therefore, we make the hypothesis that, as Ga is incorporated into the In_2O_3 matrix, its structure is distorted and, accordingly, its bandgap changes. In this way we explain the appearance of the two close and comparable PL bands by the coexistence of two separate regions of the NWs, one the crystalline core of the NW and the other one its surface shell, with a different ratio of Ga ions incorporation. If we compare the obtained gap with our Ga concentration results from the XRD analysis, displayed in figure 7, we can see that we likely have a maximum Ga concentration of about 3%, similar to what Mohamed et al. observed. However, due to the limited accuracy, a proper correlation cannot be established. Some care should be taken, however, about the fact that Ga is not the only element that could be incorporated in the NWs, modifying their crystalline structure. As previously stated, it could be possible that residual carbon atoms from the graphite source had contaminated our sample and it could be the actual cause of the structural changes.

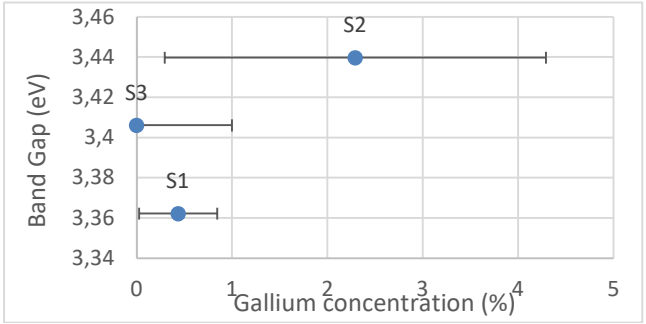

Fig 7: Dispersion of the bandgap as a function of the gallium concentration.

As for the displacement of both PL peaks from sample to sample, we found that the coherent shift correlates with the integrated intensity of the high peak divided by the short one, as can be seen in figure 9. This suggests that whatever is originating the blue peak is also causing the shift. One way to explain this would be assuming that the higher gallium (or carbon) concentration is due to a lower amount of indium, which would result in smaller NWs for both the core and shell regions, which, as observed in silicon nanocrystals [8] could result in a blue-shift of the bandgap. If this was the case, we should be able to find a correlation with the size of crystalline domains and the bandgap shift. However, as displayed in figure 8, no correlation was observed. An alternative approach to the same issue would be assuming that the stoichiometry of all samples is not the same, which, as stated by Mohamed et al. [6] could cause a shift of the band gap. This hypothesis fails to explain why the shift is the same for both peaks and would

require further analysis of the composition of the NWs, as their stoichiometry could not be measured.

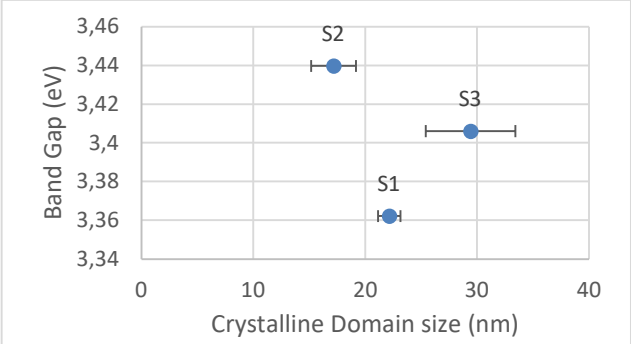

Fig 8: Dispersion of the bandgap as a function of the size of the crystalline domains in the same samples as in Fig. 7.

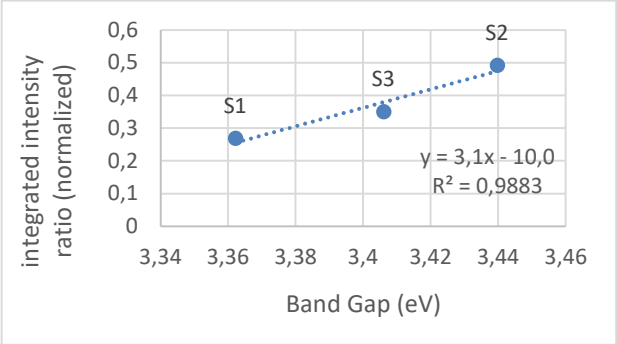

Fig 9: Dispersion of the integrated intensity ratio between peaks as a function of the the bandgap.

IV. CONCLUSIONS

In this work we have grown Ga_2O_3 NWs from a metallic source through the VLS method and analysed the effect of the carrier gas. We have found that a marginal concentration of oxygen (2ppm) is enough to completely disrupt the synthesis, as it causes oxidation of the source before evaporation.

Additionally, an in-depth analysis of $(In,Ga)_2O_3$ NWs grown from leftover In_2O_3 on the inner walls of our furnace and a C:Ga_2O_3 source was carried out. From that analysis, a correlation of the optical bandgap and the presence of an unidentified element that modifies our semiconductor nanostructures (most likely Ga or C) has been found.

Despite the efforts to relate bandgap with crystalline and chemical parameters, no correlation of neither the gallium concentration nor the crystalline domain size was found with neither the spectrum shift nor the second peak position.

At personal level, throughout this project I had a chance to make use of a wide range of knowledge gained in subjects such as solid state physics and fundamental spectroscopy, which I doubt I would have had much of a chance to put to work otherwise, as well as to a chance to, to a rather shallow extent, experience what it means to do research.

V. ACKNOWLEDGEMENTS

I would like to acknowledge Dr. Paolo Pellegrino for helping me out on about every single aspect of this project, such as the synthesis of the NWs, data analysis and bibliographic resources. I would additionally like to acknowledge Dr. Albert Romano for the invaluable insights he provided during the entire development of this work.

I would finally like to acknowledge my family for their help to cope during these harsh months and my friends for their everlasting support.

[1] A. Afzal, « β -Ga2O3 nanowires and thin films for metal oxide semiconductor gas sensors: Sensing mechanisms and performance enhancement strategies» *Journal of Materiomics,* vol. 5, pp. 542-557, 2019.

[2] Daihua Zhang et al. «Detection of NO2 down to ppb Levels Using Individual and Multiple In2O3 Nanowire Devices», *Nano Letters*, vol. 4, pp. 1919–1924, 2004.

[3] M. Kumar et al., «Diameter Tuning of β-Ga2O3 Nanowires Using Chemical Vapor Deposition Technique» *Nanoscale research letters,*vol. 12, pp. 184, 2017.

[4] L.Vegard, «Die Konstitution der Mischkristalle un die Raumfüllung der Atome», *Zeitschrift für Physik*, vol. 5, pp. 17-26, 1921.

[5] P. Scherrer, "Bestimmung der inneren Struktur un der Größe von Kolloidteilchen mittels Röntgenstrahlen," *Kolloidchemie Ein Lehrbuch*, pp. 387-409, 1912.

[6] S. H. Mohamed, « Transparent Conductive Gallium-doped Indium Oxide Nanowires for Optoelectronic Applications» *Journal of the Korean Physical Society,* vol. 62, pp. 902-905, 2013.

[7] A. Yahia et al, « Structural, optical, morphological and electrical properties of indium oxide thin films prepared by sol gel spin coating process» *Surfaces and Interfaces,* vol. 14, pp. 158-165, 2019.

[8] K. Kůsová, «Silicon Nanocrystals: From Indirect to Direct Bandgap», *Physica status solidi,* vol. 215, pp. 1700718, 2017.